# Optimization of stability and flow of modified asphalt concrete using ceramic tile waste and quarry dust

**Joseph SAMUEL** ▪ Department of Civil Engineering, University of Nigeria, Nsukka, Nigeria ▪ jsolomon234@yahoo.com

**F. O. OKAFOR** ▪ Department of Civil Engineering, University of Nigeria, Nsukka, Nigeria ▪ fidelis.okafor@unn.edu.ng

Érkezett: 2024. 03. 26. ▪ Received: 26. 03. 2024. ▪ https://doi.org/10.14382/epitoanyag-jsbcm.2024.5

**Abstract**

Ceramic wastes have contributed hugely to environmental pollution in our societies, mostly because it is non-biodegradable and not reused in any significant quantity presently. Research has confirmed the feasibility of incorporating these wastes into cement concrete and asphalt concrete production. In this study, the use of ceramic tile dust as a replacement for quarry dust in hot asphalt mix was investigated and polynomial model equations have been developed for predicting the Stability and flow of asphalt mix incorporating ceramic tile dust as a full or partial replacement for quarry dust filler. The model was formulated Using Scheffe's simplex lattice theory. 15 design points were picked from the boundaries of the simplex and tests from these design points were used for model fitting. Another 15 points were picked within the simplex and test results from these points were used for model testing. Results of the laboratory tests show that the incorporation of ceramic tile dust improves the stability and flow of the resulting asphalt mix, and this was attributed to the pozzolanic property of ceramic tile dust. The model has been tested and confirmed to be adequate based on statistical values from F-statistics, Analysis of Variance, and normal probability distribution plot of model residuals. Hence, the proposed models were adequate for the prediction/optimization of stability and flow of asphalt concrete incorporating ceramic tile dust as a partial replacement for filler.

Keywords: asphalt concrete, ceramic tile dust, Scheffe's simplex lattice, stability and flow, quarry dust

Kulcsszavak: aszfaltbeton, kerámia cseréppor, Scheffe-féle szimplex rács, stabilitás és áramlás, kőbányapor

**Joseph SAMUEL**
Ph.D. student at Department of Civil Engineering, University of Nigeria, Nsukka, Nigeria. Part-time Lecturer at University of Uyo, and Senior Civil Engineer at Ministry of Works & Fire Service, Uyo, Akwa Ibom State, Nigeria. Registered engineer at Council for the Regulation of Engineering in Nigeria (COREN). Member, Nigerian Society of Engineers. Research Interest Includes: simulation and recycled aggregate asphalt concrete.

**Fidelis O. OKAFOR**
Professor of highway and construction materials at University of Nigeria, Nsukka, Nigeria. Registered engineer at Council for the Regulation of Engineering in Nigeria (COREN). Member, Nigerian Society of Engineers. Research Interest Includes: soil, cement, and concrete materials.

## 1. Introduction

In our societies today, industrial, and domestic wastes generated yearly have contributed to huge environmental problems. Recycling these industrial waste and by-products is a key to achieving sustainable development, which should be a national priority. Some of these wastes could be recycled and used afterwards as building materials by the construction industry. To produce asphalt concrete (AC) and cement concrete (CC), many industrial wastes and by-products have been used with great advantages because of study discoveries. These materials consist of substances like fly ash [1], ground granulated blast-furnace slag [2, 3], and quarry dust [4, 5].

Industries that produce ceramic products, such as sanitary ware, earthenware, electrical insulators, bricks, floor tiles, wall tiles, and roof tiles, produce ceramic wastes. Some of these wastes are produced throughout the manufacturing process due to production errors, size discrepancies, non-standard goods, glazing errors, and more. Additionally, ceramic waste could be produced during shipping and distribution processes as well as during construction and demolition at the project site. Ceramic waste makes up about 30% of all demolition wastes [6] and continues to make up 54% of all building and demolition wastes [7]. It has been reported that up to 30% of the output of the ceramic industries is wasted [8]. These non-biodegradable wastes are not significantly recycled, instead they are dumped in landfills [9-14].

According to the research that is currently available, ceramic wastes are primarily adopted in AC either as a replacement for aggregate [15-18] or as a replacement for filler [19-21], and these practices are successful. Recycled ceramic aggregate was adopted in a study [22] to partially replace conventional aggregate in hot asphalt mix. The studies were run at both full scale in an asphalt plant and scaled quantities in a laboratory. The replacement was up to 30%. The results indicate that recycled ceramic aggregate can be used to produce hot asphalt mixtures that largely satisfy the mechanical requirements for use as road binders. The Author further stated that its addition leads to increased binder and filler contents and consequently increased indirect tensile strength and resistance to plastic deformation. In a similar study, [23] reported that replacing up to 20% conventional aggregate with recycled ceramic tiles improved the marshal stability and resilient modulus strength by 25% and 13.5% respectively. Studies on the use of ceramic waste as filler material also show positive results. For instance, in a study carried out by [24], the replacement of conventional limestone filler with ceramic waste powder improves the mechanical properties of hot asphalt mix in terms of Marshal stability, resistance to moisture, fatigue life and rutting resistance. Several other studies have also reported the improved mechanical properties of AC. This happened because of the replacement of conventional filler material with ceramic waste powder [19, 21].

Asphalt mix design and optimization are very important aspects of asphalt mix production because the properties of asphalt concrete depend on the mix proportions of the constituents. The most economical and efficient way of achieving an optimum mix is the use of statistical and mathematical procedures known as response surface methodology (RMS) [25]. RMS usually requires the formulation of model equations for responses through the design of experiments and optimization of these responses using the formulated model equations [26]. These responses are usually mechanical properties. There are presently no such model equations for asphalt mix incorporating ceramic waste as either aggregate or filler. In this study, the mathematical model equation was formulated using Scheffe's simplex lattice theory [27], for the prediction of stability and flow properties of AC with partial replacement of conventional filler material with ceramic tile dust.

## 2. Materials and methods

### 2.1 Materials

Five materials: bitumen, coarse aggregate, fine aggregate, quarry dust (GD) and ceramic tile dust (CTD) were sourced from Rivers State of Nigeria, prepared, and used in this study. To obtain CTD, waste ceramic walls and floor tiles were acquired from a ceramic tile dealer in the local Market in bags. They were mechanically crushed and sieved into the required size (passing 75 μm sieve) as determined by [23]. The fine aggregate was sourced from a river sand mining site. It was air-dried to expel moisture, then sieved with a 4.5mm sieve to eliminate undesired materials. The size separation between fine and coarse aggregate was carried out by [23]. The coarse aggregate used was granite with a maximum size of 12 mm. In this investigation, penetration grade 60/70 bitumen was acquired from a reliable company. This bitumen complied with the specifications for usage as asphaltic cement in the medium traffic category. Quarry dust material was subjected to a sieve (75 μm sieve) to obtain the required particle size as determined by [23]. Preliminary tests were carried out on the materials and the respective results were collected.

### 2.2 Methods

The following procedures were applied to achieve the aim of this study: preparation and characterization of asphalt mix constituents; design of experiment using Scheffe's simplex lattice theory; production of test samples based on the designed experiment; and testing of samples. The test results were then used to formulate and validate the required Scheffe's regression model equations. Details of the procedures are as follows.

#### 2.2.1 Design of Experiment

The Design of the experiment was based on Scheffe's simplex lattice theory. The Explanations of the principles and procedures of using the theory can be found in numerous literatures [24-29]. The asphalt mix in this study had five components and the data were to be fitted into the second-degree polynomial expression. Hence, a {5,2} simplex lattice was adopted. Scheffe's reduced polynomial for a {5,2} simplex lattice is as given in *Eq. 1* and *Eq. 2*, where $S_T$ and $F$ are the responses to be modelled which are stability and flow respectively for this study. $U_i$ are the pseudo components of the model and $\theta_i$ are the model coefficients to be determined using experimental data [24-28].

$$S_T = \theta_1U_1 + \theta_2U_2 + \theta_3U_3 + \theta_4U_4 + \theta_5U_5 + \theta_{12}U_1U_2 + \theta_{13}U_1U_3 + \theta_{14}U_1U_4 + \theta_{15}U_1U_5 + \theta_{23}U_2U_3 + \theta_{24}U_2U_4 + \theta_{25}U_2U_5 + \theta_{34}U_3U_4 + \theta_{35}U_3U_5 + \theta_{45}U_4U_5 \quad (1)$$

$$F = \theta_1U_1 + \theta_2U_2 + \theta_3U_3 + \theta_4U_4 + \theta_5U_5 + \theta_{12}U_1U_2 + \theta_{13}U_1U_3 + \theta_{14}U_1U_4 + \theta_{15}U_1U_5 + \theta_{23}U_2U_3 + \theta_{24}U_2U_4 + \theta_{25}U_2U_5 + \theta_{34}U_3U_4 + \theta_{35}U_3U_5 + \theta_{45}U_4U_5 \quad (2)$$

Generation of test data for the determination of model coefficients for a {5,2} simplex lattice polynomial requires data from at least 15 design points within the simplex [24, 26, 27]. Therefore, 15 design points were picked from the surface of the simplex for the generation of data that would be used for the model fitting. These included 5 points from the 5 vertices (*Fig. 1*) of the simplex which represented the pure blends. The remaining 10 points were selected from halfway between two vertices on the boundaries of the simplex. As control points, 15 other points (*Fig. 2*) were also selected within the simplex (not at the boundaries). Data from the control points were used for the model testing. Lower and upper boundaries for each component were taken as 0 and 1 respectively while the sum of all components at each test point equals 1. The generated design matrix in pseudo components at the design and control points are presented in *Table 1* and *Table 2* respectively.

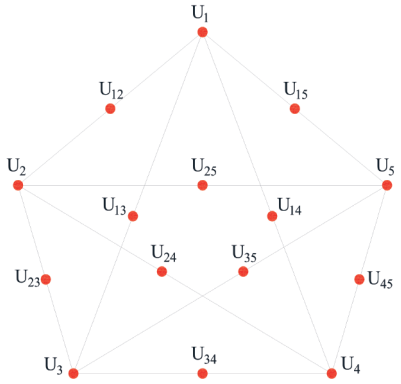


*Fig. 1 Scheffe's simplex plot for pseudo components*
*1. ábra Scheffe szimplex ábrája pszeudo komponensek esetén*

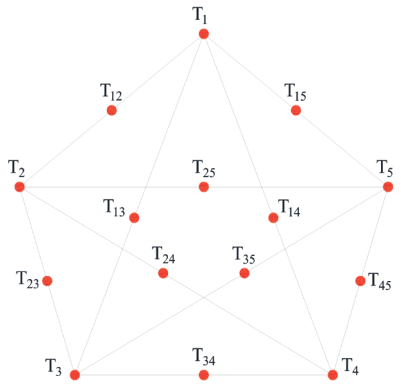


*Fig. 2 Scheffe's simplex plot for actual components*
*2. ábra Scheffe szimplex ábrája a tényleges komponensekre vonatkozóan*

| Design Points | Pseudo Component | | | | | Response | Actual component | | | | |
|---|---|---|---|---|---|---|---|---|---|---|---|
| | U1 | U2 | U3 | U4 | U5 | $v_{exp}$ | T1 Asphalt | T2 Granite | T3 Sand | T4 QD | T5 CTD |
| 1 | 1.00 | 0.00 | 0.00 | 0.00 | 0.00 | $V_1$ | 0.040 | 0.480 | 0.4608 | 0.01536 | 0.00384 |
| 2 | 0.00 | 1.00 | 0.00 | 0.00 | 0.00 | $V_2$ | 0.045 | 0.5133 | 0.4207 | 0.0126 | 0.00840 |
| 3 | 0.00 | 0.00 | 1.00 | 0.00 | 0.00 | $V_3$ | 0.050 | 0.5463 | 0.3816 | 0.0089 | 0.01330 |
| 4 | 0.00 | 0.00 | 0.00 | 1.00 | 0.00 | $V_4$ | 0.055 | 0.5788 | 0.3433 | 0.0046 | 0.01830 |
| 5 | 0.00 | 0.00 | 0.00 | 0.00 | 1.00 | $V_5$ | 0.060 | 0.611 | 0.306 | 0.0230 | 0.0000 |
| 6 | 0.50 | 0.50 | 0.00 | 0.00 | 0.00 | $V_{12}$ | 0.043 | 0.497 | 0.441 | 0.0140 | 0.0060 |
| 7 | 0.50 | 0.00 | 0.50 | 0.00 | 0.00 | $V_{13}$ | 0.045 | 0.5132 | 0.4212 | 0.0121 | 0.00857 |
| 8 | 0.50 | 0.00 | 0.00 | 0.50 | 0.00 | $V_{14}$ | 0.0475 | 0.5294 | 0.4021 | 0.0100 | 0.01107 |
| 9 | 0.50 | 0.00 | 0.00 | 0.00 | 0.50 | $V_{15}$ | 0.0500 | 0.5455 | 0.3834 | 0.0192 | 0.01075 |
| 10 | 0.00 | 0.50 | 0.50 | 0.00 | 0.00 | $V_{23}$ | 0.0475 | 0.5298 | 0.4012 | 0.0108 | 0.01085 |
| 11 | 0.00 | 0.50 | 0.00 | 0.50 | 0.00 | $V_{24}$ | 0.0500 | 0.5461 | 0.3820 | 0.0086 | 0.01335 |
| 12 | 0.00 | 0.50 | 0.00 | 0.00 | 0.50 | $V_{25}$ | 0.0525 | 0.5622 | 0.3634 | 0.0178 | 0.0042 |
| 13 | 0.00 | 0.00 | 0.50 | 0.50 | 0.00 | $V_{34}$ | 0.053 | 0.5630 | 0.3620 | 0.0070 | 0.0160 |
| 14 | 0.00 | 0.00 | 0.50 | 0.00 | 0.50 | $V_{35}$ | 0.055 | 0.5790 | 0.3440 | 0.0160 | 0.0070 |
| 15 | 0.00 | 0.00 | 0.00 | 0.50 | 0.50 | $V_{45}$ | 0.058 | 0.5950 | 0.3250 | 0.0140 | 0.0090 |

*Table 1 Design matrix showing pseudo and actual components of design points for model fitting*
*1. táblázat A tervezési mátrix, amely a modellillesztéshez használt tervezési pontok pszeudo- és tényleges összetevőit mutatja*

| Control Points | Pseudo Component | | | | | Response | Actual component | | | | |
|---|---|---|---|---|---|---|---|---|---|---|---|
| | U1 | U2 | U3 | U4 | U5 | $V_{exp}$ | T1 Asphalt | T2 Granite | T3 Sand | T4 QD | T5 CTD |
| 1 | 0.333 | 0.333 | 0.333 | 0.000 | 0.000 | $V_{C1}$ | 0.045 | 0.5132 | 0.4210 | 0.0123 | 0.0085 |
| 2 | 0.333 | 0.333 | 0.000 | 0.333 | 0.000 | $V_{C2}$ | 0.0467 | 0.5240 | 0.4082 | 0.0109 | 0.0102 |
| 3 | 0.333 | 0.000 | 0.333 | 0.333 | 0.000 | $V_{C3}$ | 0.0483 | 0.5350 | 0.3952 | 0.0096 | 0.0118 |
| 4 | 0.333 | 0.333 | 0.000 | 0.000 | 0.333 | $V_{C4}$ | 0.0483 | 0.5347 | 0.3958 | 0.0170 | 0.0041 |
| 5 | 0.250 | 0.250 | 0.250 | 0.250 | 0.000 | $V_{C5}$ | 0.0475 | 0.5296 | 0.4016 | 0.0104 | 0.01096 |
| 6 | 0.250 | 0.250 | 0.250 | 0.000 | 0.250 | $V_{C6}$ | 0.0490 | 0.5380 | 0.3920 | 0.0150 | 0.0060 |
| 7 | 0.250 | 0.250 | 0.000 | 0.250 | 0.250 | $V_{C7}$ | 0.0500 | 0.5458 | 0.3827 | 0.0139 | 0.0076 |
| 8 | 0.000 | 0.250 | 0.250 | 0.250 | 0.250 | $V_{C8}$ | 0.0525 | 0.5624 | 0.3629 | 0.0123 | 0.0100 |
| 9 | 0.300 | 0.100 | 0.200 | 0.200 | 0.200 | $V_{C9}$ | 0.0495 | 0.5426 | 0.3865 | 0.0132 | 0.0083 |
| 10 | 0.200 | 0.200 | 0.100 | 0.300 | 0.200 | $VC_{10}$ | 0.0505 | 0.5491 | 0.3787 | 0.0125 | 0.0093 |
| 11 | 0.200 | 0.200 | 0.200 | 0.100 | 0.300 | $VC_{11}$ | 0.0505 | 0.5491 | 0.3788 | 0.0148 | 0.0069 |
| 12 | 0.200 | 0.200 | 0.200 | 0.200 | 0.200 | $VC_{12}$ | 0.0500 | 0.5459 | 0.3825 | 0.0129 | 0.0088 |
| 13 | 0.150 | 0.250 | 0.200 | 0.200 | 0.200 | $VC_{13}$ | 0.0500 | 0.5480 | 0.3800 | 0.0130 | 0.0090 |
| 14 | 0.200 | 0.200 | 0.150 | 0.250 | 0.200 | $VC_{14}$ | 0.0050 | 0.5480 | 0.381 | 0.0130 | 0.0090 |
| 15 | 0.250 | 0.200 | 0.200 | 0.200 | 0.150 | $VC_{15}$ | 0.0490 | 0.5390 | 0.390 | 0.0130 | 0.0090 |

*Table 2 Design matrix showing pseudo and actual components at control points*
*2. táblázat Tervezési mátrix, amely a pszeudo és a tényleges komponenseket mutatja az ellenőrzési pontokon*

### 2.2.2 Transformation of Pseudo to Actual Components

From Scheffe's polynomial theory, the relationship between a set of pseudo components and actual components at a test point for the responses is as given in *Eq. 3* where $T$ is a column matrix of real component ratios, $U$ is a column matrix of pseudo components at a test point and $A$ is a square matrix of actual components corresponding to the pure blends at the five vertices of the simplex.

$$T = A^T U \quad (3)$$

The Mix compositions at the vertices of the simplex were selected based on the author's experience and data from the literature. From existing literature, [30, 31] the Optimum Bitumen Content (OBC) of an asphalt mix always falls between 4% - 6% of the total weight/volume of the asphalt mixture, making the aggregate content to be limited to 94% - 96% of the total mix. For aggregate combination, coarse aggregate usually falls in the range of 50% - 65% of the aggregate content; thus, limiting the fine aggregate content to 35% - 50%. Total filler content is usually limited to the range of 4% - 7% of the fine aggregate content while CTD content varies between 0% - 80% of the filler content. The ratio of bitumen ($T_1$), coarse aggregate ($T_2$), fine aggregate ($T_3$), quarry dust ($T_4$) and CTD

($T_5$) at vertex $U_1$, were therefore selected respectively as: [0.040: 0.4800: 0.4608: 0.01536: 0.00384]. Mix ratios at the other four vertices ($U_2$, $U_3$, $U_4$, and $U_5$) were selected respectively as: [0.045: 0.5133: 0.4207: 0.0126: 0.0084], [0.050: 0.5463: 0.3816: 0.0089: 0.0133], [0.055: 0.5788, 0.3433: 0.0046: 0.0183], [0.060: 0.6110: 0.3060: 0.0230: 0.0000]. By arranging these in a matrix form, the square matrix, $A$ was achieved as:

$$A = \begin{bmatrix} 0.040 & 0.480 & 0.4608 & 0.01536 & 0.00384 \\ 0.045 & 0.5133 & 0.4207 & 0.0126 & 0.0084 \\ 0.050 & 0.5463 & 0.3816 & 0.0089 & 0.0133 \\ 0.055 & 0.5788 & 0.3433 & 0.0046 & 0.0183 \\ 0.060 & 0.6110 & 0.3060 & 0.0230 & 0.0000 \end{bmatrix} \quad \text{and}$$

by transposing matrix $A$, $A^T$ was deduced as

$$A^T = \begin{bmatrix} 0.040 & 0.045 & 0.050 & 0.055 & 0.060 \\ 0.4800 & 0.5133 & 0.5463 & 0.5788 & 0.6110 \\ 0.4608 & 0.4207 & 0.3816 & 0.3433 & 0.3060 \\ 0.01536 & 0.0126 & 0.0089 & 0.0046 & 0.0230 \\ 0.00384 & 0.0084 & 0.0133 & 0.0183 & 0.0000 \end{bmatrix},$$

Substituting $A^T$ into *Eq. 2* gave

$$\begin{pmatrix} T_1 \\ T_2 \\ T_3 \\ T_4 \\ T_5 \end{pmatrix} = \begin{pmatrix} 0.040 & 0.045 & 0.050 & 0.055 & 0.060 \\ 0.4800 & 0.5133 & 0.5463 & 0.5788 & 0.6110 \\ 0.4608 & 0.4207 & 0.3816 & 0.3433 & 0.3060 \\ 0.01536 & 0.0126 & 0.0089 & 0.0046 & 0.0230 \\ 0.00384 & 0.0084 & 0.0133 & 0.0183 & 0.0000 \end{pmatrix} \begin{pmatrix} U_1 \\ U_2 \\ U_3 \\ U_4 \\ U_5 \end{pmatrix} \quad (4)$$

Transformation of pseudo components to real components was carried out using *Eq. 4* as follows:
In response $V_{12}$;

$$\begin{pmatrix} T_1 \\ T_2 \\ T_3 \\ T_4 \\ T_5 \end{pmatrix} = \begin{pmatrix} 0.040 & 0.045 & 0.050 & 0.055 & 0.060 \\ 0.4800 & 0.5133 & 0.5463 & 0.5788 & 0.6110 \\ 0.4608 & 0.4207 & 0.3816 & 0.3433 & 0.3060 \\ 0.01536 & 0.0126 & 0.0089 & 0.0046 & 0.0230 \\ 0.00384 & 0.0084 & 0.0133 & 0.0183 & 0.0000 \end{pmatrix} \begin{pmatrix} 0.5 \\ 0.5 \\ 0 \\ 0 \\ 0 \end{pmatrix} = \begin{pmatrix} 0.043 \\ 0.497 \\ 0.441 \\ 0.0140 \\ 0.006 \end{pmatrix}$$

In the same way, at response $V_{13}$,

$$\begin{pmatrix} T_1 \\ T_2 \\ T_3 \\ T_4 \\ T_5 \end{pmatrix} = \begin{pmatrix} 0.040 & 0.045 & 0.050 & 0.055 & 0.060 \\ 0.4800 & 0.5133 & 0.5463 & 0.5788 & 0.6110 \\ 0.4608 & 0.4207 & 0.3816 & 0.3433 & 0.3060 \\ 0.01536 & 0.0126 & 0.0089 & 0.0046 & 0.0230 \\ 0.00384 & 0.0084 & 0.0133 & 0.0183 & 0.0000 \end{pmatrix} \begin{pmatrix} 0.5 \\ 0 \\ 0.5 \\ 0 \\ 0 \end{pmatrix} = \begin{pmatrix} 0.045 \\ 0.5132 \\ 0.4212 \\ 0.0121 \\ 0.00857 \end{pmatrix}$$

Real components for all the design points and control points as given in *Table 1* and *Table 2*, were computed using the same procedure.

### 2.2.3 Preparation and Testing of Specimens

Hot mix Asphalt concrete was batched by weight making use of the real component ratios in *Table 1* and *Table 2*. A total of 30 different samples were prepared. 15 sample types were taken to represent design points and the results from these points were used for the model fitting while another 15 different sample types were prepared using data from the control points and their results were used for the model testing. All mixing and compaction of asphalt concrete were carried out by ASTM D8079-16 [32]. Stability and flow tests were carried out by the procedures described in ASTM D6927 [33], the standard test method for Marshall stability and flow of bituminous mixtures. Using the Marshall testing machine, the Marshall stability values were recorded when the specimens were loaded at constant strain (50.8 mm per minute) to failure and at a preheated temperature of 60 °C. While the stability test at the failure point was in progress, the dial gauge was used to measure the corresponding vertical deformations known as Marshall flow values of the specimen expressed in units of 0.25 mm.

### 2.2.3 Determination of Model Coefficients

From the principle of Scheffe's theory, the number of design points required for model fitting as shown in Table 1 must be equal to the number of model coefficients in the polynomial equation (*Eq. 1*) [24-29]. From this relationship, the coefficient of the polynomial equation can be related to the expected experimented responses at the design points as in *Eq. 5*. In this study, the model coefficients were obtained based on *Eq. 5*. using the experimental responses at the design points.

$$\theta_i = v_i \quad \text{and} \quad \theta_{ij} = 4v_{ij} - 2v_i - 2v_j \quad (5)$$

## 3. Results

### 3.1 Material characterisation

Particle size distribution of fine and coarse aggregates used in this study are given in *Fig. 3* and *4* respectively while volumetric properties of asphalt concrete components are presented in *Table 3*., *Tables 4* and *5* present the properties of bitumen used and compound compositions of CTD respectively.

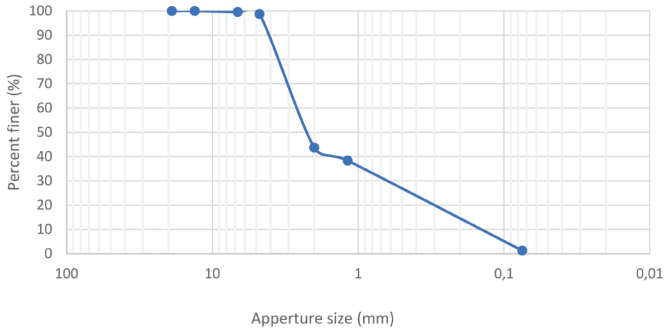


*Fig. 3 Particle size distribution curve for fine river sand*
*3. ábra Finom folyami homok szemcseméret-eloszlási görbéje*

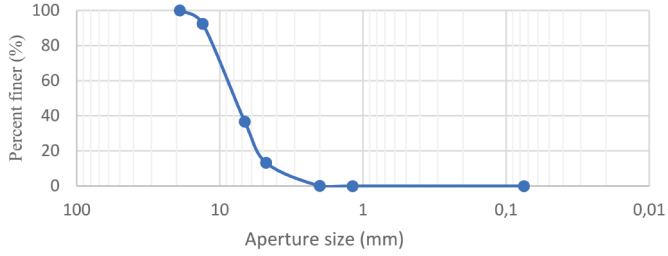


*Fig. 4 Particle size distribution curve for granite*
*4. ábra Gránit szemcseméret-eloszlási görbéje*

| Property | Sand | Granite | Bitumen | QD | CTD |
|---|---|---|---|---|---|
| **Specific gravity** | 1.64 | 2.64 | 1.04 | 1.47 | 1.18 |
| **Bulk density (kg/m³)** | 1635 | 1386 | 1040 | 1588 | 1373 |
| **Coefficient of uniformity** | 16.67 | 2.14 | | | |
| **Coefficient of gradation** | 1.13 | 1.08 | | | |

*Table 3 Asphalt concrete's component volumetric properties*
*3. táblázat Az aszfaltbeton komponenseinek térfogati tulajdonságai*

| Property | Unit | Test Method | Value |
|---|---|---|---|
| **Softening point** | °C | BS EN 1427 | 53°C |
| **Penetration** | 0.1 mm | BS EN 1426 | 68 |
| **Flash point** | °C | BS EN 22592 | 250°C |

*Table 4 Bitumen properties*
*4. táblázat A bitumen tulajdonságai*

| Compound | % Composition by mass |
|---|---|
| **$SiO_2$** | 53.57 |
| **$V_2O_5$** | 0.09 |
| **$Cr_2O_3$** | 0.09 |
| **MnO** | 0.08 |
| **$Fe_2O_3$** | 8.27 |
| **$Co_3O_4$** | 0.05 |
| **$Nb_2O_3$** | 0.01 |
| **$SO_3$** | 0.48 |
| **CaO** | 15.29 |
| **$K_2O$** | 2.94 |
| **$Al_2O_3$** | 15.47 |
| **$Ta_2O_5$** | 0.03 |
| **$TiO_2$** | 1.72 |
| **ZnO** | 0.44 |
| **BaO** | 0.22 |
| **$ZrO_2$** | 0.53 |
| **$WO_3$** | 0.01 |

*Table 5 Chemical composition of CTD*
*5. táblázat A CTD kémiai összetétele*

### 3.2 Experimental Responses for Stability and Flow

*Table 6* presents the experimental results for stability, $S_T$ and flow, $F$ of asphalt mix at the 15 design points while *Table 7* shows the same stability, $S_T$ and flow, $F$ results but with their respective pseudo and actual mix components. These values would be used for the determination of coefficients of the proposed stability, $S_T$ and flow, $F$ models. Maximum and minimum obtainable responses within the factor space of the simplex would be defined by these values. Experimental responses at the control points are also presented in *Table 8* and will be used for the model testing.

### 3.3 Model Formulation

Stability and flow experimental data from *Tables 7* and *8* were used to fit the simplex lattice polynomial model equations in *Eq. 1* based on the relationships in *Eq. 5*. The resulting model coefficients for Stability, $S_T$ were as follows: $\theta_1$=6.868; $\theta_2$=7.954; $\theta_3$=7.757; $\theta_4$=10.216; $\theta_5$=7.200; $\theta_{12}$=6.992; $\theta_{13}$=0.910; $\theta_{14}$=19.688; $\theta_{15}$=15.044; $\theta_{23}$=24.646; $\theta_{24}$=14.296; $\theta_{25}$=−1.700; $\theta_{34}$=25.726; $\theta_{35}$=−5.398; $\theta_{45}$=28.560. While that of Flow, $F$ were: $\theta_1$=4.325; $\theta_2$=3.180; $\theta_3$=3.135; $\theta_4$=5.025; $\theta_5$=5.515; $\theta_{12}$=4.850; $\theta_{13}$=8.480; $\theta_{14}$=−7.600; $\theta_{15}$=−0.800; $\theta_{23}$=1.590; $\theta_{24}$=3.710; $\theta_{25}$=−3.310; $\theta_{34}$=5.040; $\theta_{35}$=+0.980; $\theta_{45}$=−3.280. Therefore, if the five vertices of the {5,2} simplex lattice are represented in the pseudo form as $U_1$, $U_2$, $U_3$, $U_4$, and $U_5$ respectively, then the resulting Scheffe's polynomial model equations for predicting Stability, $S_T$ and Flow, $F$ are given as:

$$S_T = 6.868U_1 + 7.954U_2 + 7.757U_3 + 10.216U_4 + 7.200U_5 + 6.992U_1U_2 + 0.9100U_1U_3 + 19.688U_1U_4 + 15.044U_1U_5 + 24.646U_2U_3 + 14.296U_2U_4 - 1.700U_2U_5 + 25.726U_3U_4 - 5.398U_3U_5 + 28.560U_4U_5 \quad (6)$$

$$F = 4.325U_1 + 3.180U_2 + 3.135U_3 + 5.025U_4 + 5.515U_5 + 4.850U_1U_2 + 8.480U_1U_3 - 7.600U_1U_4 - 0.800U_1U_5 + 1.590U_2U_3 + 3.710U_2U_4 - 3.310U_2U_5 + 5.040U_3U_4 + 0.980U_3U_5 - 3.280U_4U_5 \quad (7)$$

| S/N | Stability factor | No of Stability deflections (0.042kN) | | Stability (kN) | | Average stability (kN) | Corrected stability (kN) | No of flow deflections (0.01mm) | | Flow (mm) | | Average flow (mm) | Time to failure (s) | |
|---|---|---|---|---|---|---|---|---|---|---|---|---|---|---|
| | | a | b | a | b | | ST | a | b | a | b | F | a | b |
| **V1** | 0.948 | 160 | 185 | 6.720 | 7.770 | 7.245 | 6.868 | 347.4 | 347.0 | 3.474 | 3.470 | 3.472 | 12.480 | 15.320 |
| **V2** | 0.855 | 194 | 249 | 8.148 | 10.458 | 9.303 | 7.954 | 268.3 | 288.3 | 2.683 | 2.883 | 2.783 | 11.970 | 13.110 |
| **V3** | 0.861 | 175 | 254 | 7.350 | 10.668 | 9.009 | 7.757 | 218.6 | 238.6 | 2.186 | 2.386 | 2.286 | 16.240 | 14.550 |
| **V4** | 0.849 | 270 | 303 | 11.340 | 12.726 | 12.033 | 10.216 | 250.6 | 230.6 | 2.506 | 2.306 | 2.406 | 16.240 | 12.240 |
| **V5** | 0.855 | 195 | 206 | 8.190 | 8.652 | 8.421 | 7.200 | 310.5 | 316.5 | 3.105 | 3.165 | 3.135 | 14.290 | 10.930 |
| **V6** | 0.874 | 265 | 234 | 11.130 | 9.828 | 10.479 | 9.159 | 225.8 | 245.8 | 2.258 | 2.458 | 2.358 | 15.820 | 14.190 |
| **V7** | 0.880 | 185 | 223 | 7.770 | 9.366 | 8.568 | 7.540 | 210.0 | 250.0 | 2.100 | 2.500 | 2.300 | 13.360 | 12.480 |
| **V8** | 0.912 | 398 | 305 | 16.716 | 12.810 | 14.763 | 13.464 | 284.3 | 264.3 | 2.843 | 2.643 | 2.743 | 10.900 | 11.920 |
| **V9** | 0.981 | 244 | 280 | 10.248 | 11.760 | 11.004 | 10.795 | 227.0 | 223.0 | 2.270 | 2.230 | 2.250 | 11.600 | 13.950 |
| **V10** | 0.973 | 330 | 356 | 13.860 | 14.952 | 14.406 | 14.017 | 330.1 | 310.1 | 3.301 | 3.101 | 3.201 | 12.070 | 10.670 |
| **V11** | 1.003 | 237 | 364 | 9.954 | 15.288 | 12.621 | 12.659 | 317.0 | 319.0 | 3.170 | 3.190 | 3.180 | 14.840 | 12.180 |
| **V12** | 0.880 | 185 | 202 | 7.770 | 8.484 | 8.127 | 7.152 | 383.1 | 379.1 | 3.831 | 3.791 | 3.811 | 9.550 | 10.990 |
| **V13** | 1.003 | 380 | 352 | 15.960 | 14.784 | 15.372 | 15.418 | 281.5 | 291.5 | 2.815 | 2.915 | 2.865 | 10.300 | 10.600 |
| **V14** | 0.813 | 179 | 180 | 7.518 | 7.560 | 7.539 | 6.129 | 337.2 | 317.2 | 3.372 | 3.172 | 3.272 | 15.770 | 12.220 |
| **V15** | 0.941 | 368 | 434 | 15.456 | 18.228 | 16.842 | 15.848 | 370.6 | 376.6 | 3.706 | 3.766 | 3.736 | 11.270 | 13.180 |

*Table 6 Stability and flow experimental test results at design points*
*6. táblázat Stabilitási és áramlási kísérletek vizsgálati eredményei a tervezési pontokon*

| N | Pseudo Component | | | | | Actual component | | | | | | |
|---|---|---|---|---|---|---|---|---|---|---|---|---|
| | $U_1$ | $U_2$ | $U_3$ | $U_4$ | $U_5$ | $T_1$ | $T_2$ | $T_3$ | $T_4$ | $T_5$ | Stability (kN) | Flow (mm) |
| $V_1$ | 1 | 0 | 0 | 0 | 0 | 0.040 | 0.480 | 0.4608 | 0.01536 | 0.00384 | 6.868 | 3.472 |
| $V_2$ | 0 | 1 | 0 | 0 | 0 | 0.045 | 0.5133 | 0.4207 | 0.0126 | 0.00840 | 7.954 | 2.783 |
| $V_3$ | 0 | 0 | 1 | 0 | 0 | 0.050 | 0.5463 | 0.3816 | 0.0089 | 0.01330 | 7.757 | 2.286 |
| $V_4$ | 0 | 0 | 0 | 1 | 0 | 0.055 | 0.5788 | 0.3433 | 0.0046 | 0.01830 | 10.216 | 2.406 |
| $V_5$ | 0 | 0 | 0 | 0 | 1 | 0.060 | 0.611 | 0.306 | 0.0230 | 0.0000 | 7.200 | 3.135 |
| $V_6$ | 0.5 | 0.5 | 0 | 0 | 0 | 0.043 | 0.497 | 0.441 | 0.0140 | 0.0060 | 9.159 | 2.358 |
| $V_7$ | 0.5 | 0 | 0.5 | 0 | 0 | 0.045 | 0.5132 | 0.4212 | 0.0121 | 0.00857 | 7.540 | 2.300 |
| $V_8$ | 0.5 | 0 | 0 | 0.5 | 0 | 0.0475 | 0.5294 | 0.4021 | 0.0100 | 0.01107 | 13.464 | 2.743 |
| $V_9$ | 0.5 | 0 | 0 | 0 | 0.5 | 0.0500 | 0.5455 | 0.3834 | 0.0192 | 0.01075 | 10.795 | 2.250 |
| $V_{10}$ | 0 | 0.5 | 0.5 | 0 | 0 | 0.0475 | 0.5298 | 0.4012 | 0.0108 | 0.01085 | 14.017 | 3.201 |
| $V_{11}$ | 0 | 0.5 | 0 | 0.5 | 0 | 0.0500 | 0.5461 | 0.3820 | 0.0086 | 0.01335 | 12.659 | 3.180 |
| $V_{12}$ | 0 | 0.5 | 0 | 0 | 0.5 | 0.0525 | 0.5622 | 0.3634 | 0.0178 | 0.0042 | 7.152 | 3.811 |
| $V_{13}$ | 0 | 0 | 0.5 | 0.5 | 0 | 0.053 | 0.5630 | 0.3620 | 0.0070 | 0.0160 | 15.418 | 2.865 |
| $V_{14}$ | 0 | 0 | 0.5 | 0 | 0.5 | 0.055 | 0.5790 | 0.3440 | 0.0160 | 0.0070 | 6.129 | 3.272 |
| $V_{15}$ | 0 | 0 | 0 | 0.5 | 0.5 | 0.058 | 0.5950 | 0.3250 | 0.0140 | 0.0090 | 15.848 | 3.736 |

*Table 7 Stability and flow test trial mix results with pseudo and actual components at design points*
*7. táblázat Stabilitási és áramlási próbakeverékek eredményei pszeudo- és tényleges komponensekkel a tervezési pontokon*

| N | Pseudo Component | | | | | Actual component | | | | | Response Symbol | Experimented $S_T$ (kN) | Experimented $F$ (mm) |
|---|---|---|---|---|---|---|---|---|---|---|---|---|---|
| | $U_1$ | $U_2$ | $U_3$ | $U_4$ | $U_5$ | $T_1$ | $T_2$ | $T_3$ | $T_4$ | $T_5$ | | | |
| 1 | 0.333 | 0.333 | 0.333 | 0.000 | 0.000 | 0.0450 | 0.5132 | 0.4210 | 0.0123 | 0.0085 | VC1 | 11.697 | 2.502 |
| 2 | 0.333 | 0.333 | 0.000 | 0.333 | 0.000 | 0.0467 | 0.5240 | 0.4082 | 0.0109 | 0.0102 | VC2 | 12.536 | 2.712 |
| 3 | 0.333 | 0.000 | 0.333 | 0.333 | 0.000 | 0.0483 | 0.5350 | 0.3952 | 0.0096 | 0.0118 | VC3 | 13.156 | 2.617 |
| 4 | 0.333 | 0.333 | 0.000 | 0.000 | 0.333 | 0.0483 | 0.5347 | 0.3958 | 0.0170 | 0.0041 | VC4 | 9.399 | 2.692 |
| 5 | 0.250 | 0.250 | 0.250 | 0.250 | 0.000 | 0.0475 | 0.5296 | 0.4016 | 0.0104 | 0.0110 | VC5 | 13.368 | 2.717 |
| 6 | 0.250 | 0.250 | 0.250 | 0.000 | 0.250 | 0.0490 | 0.5380 | 0.3920 | 0.0150 | 0.0060 | VC6 | 9.815 | 2.802 |
| 7 | 0.250 | 0.250 | 0.000 | 0.250 | 0.250 | 0.0500 | 0.5458 | 0.3827 | 0.0139 | 0.0076 | VC7 | 13.288 | 3.063 |
| 8 | 0.000 | 0.250 | 0.250 | 0.250 | 0.250 | 0.0525 | 0.5624 | 0.3629 | 0.0123 | 0.0100 | VC8 | 13.597 | 3.697 |
| 9 | 0.300 | 0.100 | 0.200 | 0.200 | 0.200 | 0.0495 | 0.5426 | 0.3865 | 0.0132 | 0.0083 | VC9 | 12.821 | 2.805 |
| 10 | 0.200 | 0.200 | 0.100 | 0.300 | 0.200 | 0.0505 | 0.5491 | 0.3787 | 0.0125 | 0.0093 | VC10 | 13.417 | 3.128 |
| 11 | 0.200 | 0.200 | 0.200 | 0.100 | 0.300 | 0.0505 | 0.5491 | 0.3788 | 0.0148 | 0.0069 | VC11 | 12.047 | 3.064 |
| 12 | 0.200 | 0.200 | 0.200 | 0.200 | 0.200 | 0.0500 | 0.5459 | 0.3825 | 0.0129 | 0.0088 | VC12 | 13.337 | 3.025 |
| 13 | 0.150 | 0.250 | 0.200 | 0.200 | 0.200 | 0.0500 | 0.5480 | 0.3800 | 0.0130 | 0.0090 | VC13 | 13.396 | 3.127 |
| 14 | 0.200 | 0.200 | 0.150 | 0.250 | 0.200 | 0.0050 | 0.5480 | 0.3810 | 0.0130 | 0.0090 | VC14 | 13.741 | 3.091 |
| 15 | 0.250 | 0.200 | 0.200 | 0.200 | 0.150 | 0.0490 | 0.5390 | 0.3900 | 0.0130 | 0.0090 | VC15 | 13.878 | 2.913 |

*Table 8 Stability (ST) and flow (F) and corresponding pseudo and actual components at control points*
*8. táblázat Stabilitás (ST) és áramlás (F), valamint a megfelelő pszeudo és tényleges komponensek az ellenőrzési pontokon*

### 3.4 Model Validation

*Table 9* shows model residuals which is the difference between the respective experimental response and model predicted response of stability and flow, while *Fig. 5* and *6* show a normal probability plot of the same model residuals for stability and flow respectively. The test of the adequacy of the proposed stability and flow models was carried out using the F-test and Analysis of Variance based on experimental and model-predicted responses at the 15 control points. *Tables 10* and *12* present the result of the F-test while *Tables 11* and *13* show the results of the Analysis of Variance for stability and flow respectively. The null hypothesis for both tests was that there is no significant difference between experimental and model-predicted responses at the control points while the alternative hypothesis was that there is a significant difference between the two sets of values. From the F-Test results in *Tables 10* and *12*, the F-value for stability and flow are 1.030 and 1.058 respectively, and less than the corresponding F-Critical values which are 2.484 and 2.484. These indicate that the null hypothesis for the two tests can not be rejected. Thus, there was no significant difference between the experimental responses and their respective model-predicted responses. Thus, there was no significant difference between the experimental responses and their respective model-predicted responses. Statistics from the result of the Analysis of Variance test for stability and flow in *Tables 11* and *13* also show that F-values (0.058 and 0.0033 respectively) are less than the corresponding

| Control Point | Stability, ST (kN) | | | | Flow, F (mm) | | | |
|---|---|---|---|---|---|---|---|---|
| | Experimental Response | Predicted Response | Residual | % Error | Experimental Response | Predicted Response | Residual | % Error |
| $V_{C1}$ | 11.367 | 11.143 | 0.224 | 1.973 | 2.502 | 2.544 | -0.042 | 1.674 |
| $V_{C2}$ | 12.857 | 12.899 | -0.042 | 0.330 | 2.712 | 2.718 | -0.006 | 0.225 |
| $V_{C3}$ | 13.497 | 13.427 | 0.070 | 0.519 | 2.617 | 2.608 | 0.009 | 0.361 |
| $V_{C4}$ | 9.551 | 9.600 | -0.049 | 0.512 | 2.692 | 2.698 | -0.006 | 0.239 |
| $V_{C5}$ | 13.940 | 13.965 | -0.025 | 0.181 | 2.717 | 2.793 | -0.077 | 2.830 |
| $V_{C6}$ | 9.914 | 9.975 | -0.061 | 0.613 | 2.802 | 2.839 | -0.037 | 1.303 |
| $V_{C7}$ | 13.839 | 13.239 | 0.600 | 4.335 | 3.063 | 3.045 | 0.018 | 0.588 |
| $V_{C8}$ | 13.617 | 13.665 | -0.048 | 0.352 | 3.697 | 3.690 | 0.007 | 0.189 |
| $V_{C9}$ | 12.922 | 12.939 | -0.017 | 0.130 | 2.805 | 2.850 | -0.045 | 1.597 |
| $V_{C10}$ | 14.119 | 13.986 | 0.133 | 0.940 | 3.128 | 3.112 | 0.016 | 0.497 |
| $V_{C11}$ | 11.740 | 11.527 | 0.213 | 1.816 | 3.064 | 3.055 | 0.008 | 0.274 |
| $V_{C12}$ | 13.147 | 13.149 | -0.002 | 0.015 | 3.025 | 3.065 | -0.040 | 1.313 |
| $V_{C13}$ | 13.285 | 13.202 | 0.083 | 0.622 | 3.127 | 3.195 | -0.068 | 2.183 |
| $V_{C14}$ | 13.849 | 13.632 | 0.217 | 1.564 | 3.091 | 3.094 | -0.003 | 0.090 |
| $V_{C15}$ | 13.121 | 13.157 | -0.036 | 0.278 | 2.913 | 2.935 | -0.022 | 0.761 |

*Table 9 Model residuals for Stability and Flow at control points*
*9. táblázat A stabilitásra és az áramlásra vonatkozó modell maradékai az ellenőrzési pontokon*

F-critical values (4.196 and 4.196), and their P-values (0.811 and 0.857) are greater than 0.05. Hence, the proposed model is adequate for the prediction of stability and flow of asphalt concrete incorporating CTD as partial replacement for filler.

| | Experimental Response | Predicted Response |
|---|---|---|
| **Mean** | 12.758 | 12.634 |
| **Variance** | 2.016 | 1.957 |
| **Observations** | 15.000 | 15.000 |
| **df** | 14.000 | 14.000 |
| **F** | 1.030 | |
| **P(F<=f) one-tail** | 0.478 | |
| **F Critical one-tail** | 2.484 | |
| **Mean** | 12.758 | 12.634 |
| **Variance** | 2.016 | 1.957 |
| **Observations** | 15.000 | 15.000 |
| **df** | 14.000 | 14.000 |

*Table 10 F-test result for experimental response and model predicted response of Stability at control points*
*10. táblázat F-próba eredménye a kísérleti válasz és a modell által megjósolt stabilitás válaszára az ellenőrzési pontokon*

| Groups | Count | Sum | Average | Variance | | |
|---|---|---|---|---|---|---|
| Experimental flow | 15.000 | 191.365 | 12.758 | 2.016 | | |
| Predicted Model | 15.000 | 189.505 | 12.634 | 1.957 | | |
| **Source of Variation** | **Sum of Square** | **Degree of Freedom** | **Mean Square** | **F-value** | **P-value** | **F crit** |
| Between Groups | 0.115 | 1.000 | 0.115 | 0.058 | 0.811 | 4.196 |
| Within Groups | 55.627 | 28.000 | 1.987 | | | |
| Total | 55.743 | 29.000 | | | | |

*Table 11 Analysis of Variance (single factor) for experimental and model response of Stability at control points*
*11. táblázat. Varianciaanalízis (egytényezős) a stabilitás kísérleti és modellválaszára az ellenőrzési pontoknál*

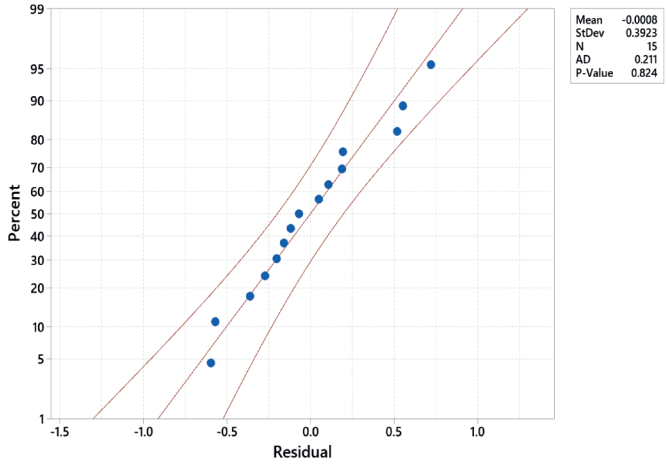


*Fig. 5 Normal probability plot of stability model residuals at control points*
*5. ábra A stabilitási modell maradványainak normál valószínűségi ábrája az ellenőrzési pontokon*

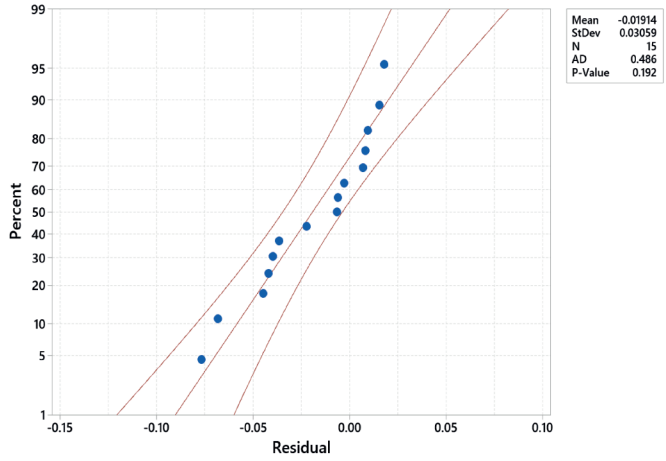


*Fig. 6 Normal probability plot of flow model residuals at control points*
*6. ábra Az áramlási modell maradványainak normál valószínűségi ábrája az ellenőrzési pontokon*

| | Experimental Response | Predicted Response |
|---|---|---|
| **Mean** | 2.930 | 2.949 |
| **Variance** | 0.086 | 0.081 |
| **Observations** | 15 | 15 |
| **df** | 14 | 14 |
| **F** | 1.058 | |
| **P(F<=f) one-tail** | 0.459 | |
| **F Critical one-tail** | 2.484 | |
| **Mean** | 2.930 | 2.949 |
| **Variance** | 0.086 | 0.081 |
| **Observations** | 15 | 15 |
| **df** | 14 | 14 |

*Table 12 F - test result for experimental response and model predicted response of flow at control points*
*12. táblázat F - a kísérleti válasz és a modell által előre jelzett áramlási válasz vizsgálati eredménye az ellenőrzési pontokon*

| Groups | Count | Sum | Average | Variance |
|---|---|---|---|---|
| **Experimental flow** | 15 | 43.954 | 2.930 | 0.086 |
| **Predicted Model** | 15 | 44.241 | 2.949 | 0.081 |

| Source of Variation | Sum of Square | Degree of Freedom | Mean Square | F - value | P-value | F crit |
|---|---|---|---|---|---|---|
| **Between Groups** | 0.003 | 1.000 | 0.003 | 0.033 | 0.857 | 4.196 |
| **Within Groups** | 2.334 | 28.000 | 0.083 | | | |
| **Total** | 2.337 | 29.000 | | | | |

*Table 13 Analysis of Variance (single factor) for experimental and model response of flow at control points*
*13. táblázat Varianciaanalízis (egytényezős) az áramlás kísérleti és modellválaszára az ellenőrzési pontoknál*

## 4. Discussion

From *Table 3*, the specific gravity and bulk density of CTD are 1.18 and 1373 kg/m$^3$ while the respective values for sand are 1.47 and 1588 kg/m$^3$. These values show that the specific gravity and bulk density of CDT are slightly lower than those of QD indicating that CTD is a lighter filler material than QD. This tends to enhance the cohesion of the asphalt mix. Results from *Figures 3* and *4* of the uniformity coefficient and coefficient of gradation show that both fine aggregate and coarse aggregate used are well-graded. This is because their uniformity coefficients were greater than 4.0 and their coefficient of gradation is between 1.0 and 3.0 [34]. Using well-graded aggregates also ensures the production of asphalt mix with good performance because aggregate gradation affects the performance of resulting asphalt concrete and cement concrete [35].

From *Tables 7* and *8*, it could be observed that asphalt mix with a high percentage of CTD is characterised by high stability and the corresponding flow. This shows that the incorporation of CTD as filler improves the stability and flow of the resulting asphalt mix. This is not surprising because it has been reported elsewhere [15, 36]. The chemical composition of CTD as presented in *Table 5* is typical of ceramic waste materials [24, 27, 37] and possesses $SiO_2$, $Fe_2O_3$, CaO and $Al_2O_3$ as the major oxides. The presence of these compounds indicates that there are traces of tricalcium silicate, dicalcium silicate, tricalcium aluminate and tetracalcium aluminoferrite, and this is likely to be responsible for the pozzolanic property of CTD [36] which enhanced bonding in asphalt mix and hence is responsible for the improved stability and flow.

Using Scheffe's simplex lattice theory, the polynomial model equations have been formulated for predicting the stability and flow of asphalt mix incorporating CDT as a partial replacement for QD filler. The models have been tested and confirmed to be adequate based on statistical values from the F-test and Analysis of Variance. As additional confirmation, the normal probability plots of stability and flow in *Figures 5* and *6* respectively show close distribution of the model residuals along the reference line and the respective plots have P-values of 0.824 and 0.192 which are far greater than the alpha level of 0.05. Hence the null hypothesis – that the model residuals follow a normal distribution – cannot be rejected and this justifies the use of Analysis of Variance [24, 27]. The quality of the proposed models can also be seen when comparing the percentage difference between experimental responses and their respective predicted model responses at the control points as presented in *Table 9*. The differences are generally low with the highest value being 4.335% and 2.83% for stability and flow respectively.

## 5. Conclusion

In this study, the use of CTD as a replacement for QD in hot asphalt mix has been investigated. Results of laboratory tests show that the incorporation of CTD improves the stability and flow of the resulting asphalt mix, and this is attributed to the pozzolanic property of CTD which enhances bonding and hence reduces void ratio. Using Scheffe's simplex lattice theory, polynomial model equations have been formulated for predicting the stability and flow of asphalt mix incorporating CDT as a partial replacement for QD filler. The models have been tested and confirmed to be adequate based on the statistical values from the F-Test, Analysis of Variance, and normal probability distribution plot of model residuals.

## Acknowledgement

The authors acknowledge no financial support from any organisation for the PhD studies of Joseph Samuel.

**Reference**


[1] Woszuk, A., Bandura, L., Franus, W. (2019). Fly ash a low cost and environmentally friendly filler and its effect on the properties of flexible pavement. *Journal of Cleaner Production*. 235: 493-502.

[2] Sinha, S. & Mahto, S. K. (2022). Application of marble dust and ground granulated blast-furnace slag in emulsified asphalt warm mixture. *Journal of Cleaner Production*. https://doi.org/10.1016/j.jclepro. 2022.133532

[3] Ambrose, E. E. & Forth, J. P. (2018). Influence of relative humidity on tensile and compressive creep of concrete amended with ground granulated blast-furnace slag. *Nigerian Journal of Technology*. 37 (1): 19-27.

[4] Oba, K. M. (2019). A mathematical model to predict the tensile strength of asphalt concrete using quarry dust fillers. *International Journal of Science & Engineering Research*. 10 (2): 1491-1498.

[5] Ambrose, E. E., Ekpo, D. U., Umoren, I. M., & Ekwere, U. S. (2018). Compressive strength and workability of laterised quarry sand concrete. *Nigerian Journal of Technology*. 37 (3): 605-610.

[6] Oikonomou, N. D. (2005). Recycled concrete aggregates. *Cement and Concrete Composite*. 27(2): pp.315-318.

[7] Shruthi, H. G., Gowtham, M. E., Samreen, T. and Syed, R. P. (2016). Reuse of ceramic wastes as aggregate in concrete. *International Research Journal of Engineering and Technology*, 3(7): 115-119.

[8] Senthamarai, R. M. and Devadas, M. P. (2005). Concrete with waste aggregate. *Cement and Concrete Composite,* 27: pp.910-913.

[9] Halicka, A., Ogrodnik, P., & Zegardlo, B. (2013). Using ceramic sanitary ware waste as concrete aggregate. *Construction and Building Materials.* 48: 295-305. https://doi.org/10.1016/j.conbuildmat. 2013.06.063.

[10] Vaghadia, B. K., & Bhatt, M. R. (2016). A study on the effect of waste ceramic tiles in flexible pavement. *International Journal of Advance Engineering and Research Development*. 3 (10): 26-28.

[11] Onyia, M. E., Ambrose, E. E., Okafor, F. O., Udo, J. J. (2023). Mathematical modelling of compressive strength of recycled ceramic tile concrete using modified regression theory. *Journal of Applied Science and Environmental Management.* 27 (1): 33-42.

[12] Patel, J. V., Varia, H. R., & Mishra, C. B. (2017). Design of bituminous mix with and without partial replacement of waste ceramic tiles material. *International Journal of Engineering Research and Technology.* 6(4): 725-755.

[13] Ambrose, E. E., Ogirigbo, O. R., Ekop, I. E. (2023). Compressive strength and resistance to sodium sulphate attack of concrete incorporated with fine aggregate recycled ceramic tiles. *Journal of Applied Science and Environmental Management*. 27 (3): 465-468.

[14] Huang, Q., Qian, Z., Hu, J., & Zheng, D. (2020). Evaluation of stone mastic asphalt containing ceramic waste aggregate for cooling asphalt pavement. *Materials*. 13(13), 2964.

[15] Silvestre, R., Medel, E., García, A., Navas, J. (2013). Use of ceramic wastes from the tile industry as a partial substitute for natural aggregate in hot mix asphalt binder courses. *Construction and Building Materials*. 45: 115-122.

[16] Muniandy, R., Ismail, D. H., Hassim, S. (2017). Performance of recycled ceramic waste as aggregate in hot mix asphalt (HMA). *Journal of Material Cycles and Waste Management*. https://doi.org/10.1007/s10163-017-0645-x

[17] Kara, C., Karacasu, M. (2017). Investigation of waste ceramic tile additive in hot mix asphalt using fuzzy logic approach. *Construction and Building Materials*. 141: 598-607.

[18] Olugbenga, O. J. (2019). Utilization of industrial waste products in the production of asphalt concrete for road construction. *Slovak Journal of Civil Engineering*. 27(4): 11-17.

[19] Fatima, E, Sahu, S., Jhamb, A., Kumar, R. (2014). Use of ceramic waste as filler in semi-dense bituminous concrete. *American Journal of Civil Engineering and Architecture*. 2(3): 102-106.

[20] Shamsaei, M., Khafajeh, R., Tehrani, H. G., Aghayan, I. (2019). Experimental evaluation of ceramic waste filler in hot mix asphalt. *Clean Technologies and Environmental Policy*. https://doi.org/10.1007/s10098-019-01788-9

[21] Serin, S., Onal, Y., Kayadelen, C., Morova, N. (2023). Utilization of recycled concrete and ceramic waste as filling materials in hot mix asphalt. *Periodica Polytechnica Civil Engineering*. https://doi.org/10.3311/PPci.21352

[22] Anya, U. C. (2015). Models for predicting the structural characteristics of sand-quarry dust blocks [dissertation]. Nsukka, Nigeria: University of Nigeria.

[23] EN-EUROPÄISCHE, N. O. R. M. (1995). Tests for Geometrical Properties of Aggregates. Part 2: Determination of Particle Size Distribution. Test sieves, nominal size of apertures. Bruxelles. Test Designation: EN, 933-2.

[24] Ambrose, E. E., Okafor, F. O., & Onyia, M. E. (2021). Scheffe's models for optimization of tensile and flexural strength of recycled ceramic tile aggregate concrete. *Engineering and Applied Science Research.* 48 (5): 497-508.

[25] Attah, I. C., Okafor, F. O., & Ugwu, O. O. (2021). Optimization of California bearing ratio of tropical black clay soil treated with cement kiln dust and metakaolin blend. *International Journal of Pavement Research and Technology.* 14: 655-667.

[26] Akhnazarova, S., & Kafarov, V. (1982): Experiment Optimization in Chemistry and Chemical Engineering, MIR Publishers, Moscow.

[27] Ambrose, E. E., Okafor, F. O., & Onyia, M. E. (2021). Compressive strength and Scheffe's optimization of mechanical properties of recycled ceramics tile aggregate concrete. *Epitoanyag-Journal of Silicate Based & Composite Materials.* 73 (3): 91 - 102. https://doi.org/10.14382/epitoanyag-jsbcm.2021.14

[28] Attah, I. C. – Etim, R. K. – George, U. A. – Bassey, O. B. (2020); Optimization of mechanical properties of rice husk ash concrete using Scheffe's theory, *SN Applied Sciences*, Vol. 2 p.928. https://doi.org/10.1007/s42452-020-2727-y.

[29] Attah, I. C. – Etim, R. K. – George, U. A. – Bassey, O. B. (2020); Optimization of mechanical properties of rice husk ash concrete using Scheffe's theory, *SN Applied Sciences*, https://doi.org/10.1007/s42452-020-2727-y.

[30] Oba, K. M. (2019). A mathematical model to predict the tensile strength of asphalt concrete using quarry dust filler. *International Journal of Scientific and Engineering Research.* 10(2): 1491-1498.

[31] Eme, D. B., Nwaobakata C., & Ohwerhi, K. E. (2020). Prediction of Stability and Flow Properties of Hot Mix Asphalt Using Cement as a Filler Material. *IOSR Journal of Mechanical and Civil Engineering (IOSR-JMCE), Volume 17, Issue 1, PP 44-51.*

[32] ASTM D8079-16 - Standard Practice for Preparation of Compacted Slab Asphalt Mix Samples Using a Segmented Rolling Compactor

[33] ASTM D6931-17 - Standard Test Method for Indirect Tensile (IDT) Strength of Asphalt Mixtures

[34] Ambrose, E. E., Etim, R. K., Koffi, N. E. (2019). Quality Assessment of commercially produced concrete blocks in part of Akwa Ibom State. Nigeria, *Nigerian Journal of Technology. 38 (3): 586-593.*

[35] Mkpaidem, N. U., Ambrose, E. E., Olutoge, F. A., Afangideh, C. B. (2022). Effect of coarse aggregate size and gradation on workability and compressive strength of plain concrete. *Journal of Applied Science and Environmental Management. 26 (4): 719-723.*

[36] Usanga, I. N., Okafor, F. O., Ikeagwuani, C. C. (2023). Investigation of the performance of hot mix asphalt mix enhanced with calcined marl dust used as filler. *International Journal of Pavement Research and Technology*. https://doi.org/10.1007/s42947-023-00323-w

[37] Subasi, S., Ozturk, H., Emiroglu, M. (2017). Utilization of waste ceramic powders as filler materials in self-consolidating concrete. *Construction and Building Materials.* 149: 567-574.



Ref.:
**Samuel**, Joseph – **Okafor**, F. O: *Optimization of stability and flow of modified asphalt concrete using ceramic tile waste and quarry dust* Építőanyag – Journal of Silicate Based and Composite Materials, Vol. 76, No. 2 (2024), 44–52 p. https://doi.org/10.14382/epitoanyag-jsbcm.2024.5